*Journal of Biophotonics*

JOURNAL OF BIOPHOTONICS

RESEARCH ARTICLE

# A Stand-Off Laser-Induced Breakdown Spectroscopy (LIBS) System for Remote Bacteria Identification

Yong Cheng[1,2] | Shuqing Wang[3] | Fei Chen[1,2] | Jiahui Liang[1,2] | Yan Zhang[4] | Lei Zhang[1,2] | Wangbao Yin[1,2] | Suotang Jia[1,2] | Liantuan Xiao[1,2]

[1]State Key Laboratory of Quantum Optics and Quantum Optics Devices, Institute of Laser Spectroscopy, Shanxi University, Taiyuan, China | [2]Collaborative Innovation Center of Extreme Optics, Shanxi University, Taiyuan, China | [3]SINOPEC Research Institute of Petroleum Processing Co., Ltd, Beijing, China | [4]School of Optoelectronic Engineering, Xi'an Technological University, Xi'an, China

**Correspondence:** Lei Zhang (k1226@sxu.edu.cn)

**Received:** 18 July 2024 | **Revised:** 30 August 2024 | **Accepted:** 9 September 2024

**Funding:** This study was supported by National Energy R&D Center of Petroleum Refining Technology; the National Key R&D Program of China (No. 2017YFA0304203); Changjiang Scholars and Innovative Research Team in the University of Ministry of Education of China (IRT_17R70); the National Natural Science Foundation of China (Nos. 11434007, 61975103, 61875108, and 61775125); Major Special Science and Technology Projects in Shanxi (No. 201804D131036); 111 Project (No. D18001); Fund for Shanxi '1331KSC'.

**Keywords:** bacteria | laser-induced breakdown spectroscopy (LIBS) | machine learning | remote distance

## ABSTRACT

Bacteria are the primary cause of infectious diseases, making rapid and accurate identification crucial for timely pathogen diagnosis and disease control. However, traditional identification techniques such as polymerase chain reaction and loop-mediated isothermal amplification are complex, time-consuming, and pose infection risks. This study explores remote (~3 m) bacterial identification using laser-induced breakdown spectroscopy (LIBS) with a Cassegrain reflective telescope. Principal component analysis (PCA) was employed to reduce the dimensionality of the LIBS spectral data, and the accuracy of support vector machine (SVM) and Random Forest (RF) algorithms was compared. Multiple repeated experiments showed that the RF model achieved a classification accuracy, recall, precision, and *F*1-score of 99.81%, 99.80%, 99.79%, and 0.9979, respectively, outperforming the SVM model and providing more accurate remote bacterial identification. The method based on laser-induced plasma spectroscopy and machine learning has broad application prospects, supporting noncontact disease diagnosis, improving public health, and advancing medical research and technological development.

## 1 | Introduction

Since the 20th century, diseases caused by microorganisms such as bacteria, fungi, and parasites have become a significant factor in the decline of biological populations. In the medical field, the diversity of bacteria presents immense challenges for treatment. The inability to rapidly and accurately identify pathogenic bacteria inevitably leads to delays in treatment, and there is also a risk of secondary infection during close-contact identification. Currently, common methods for bacterial identification include nucleic acid-based techniques such as polymerase chain reaction (PCR) [1] and Loop-Mediated Isothermal Amplification (LAMP) [2]. Although these methods offer high detection accuracy [3–5], they also have drawbacks, such as the potential for false positives or false negatives, complex procedures, and lengthy processing times, which fail to meet the need for rapid bacterial identification. Therefore, there is an urgent need for a fast, sensitive, safe, and remote microbial identification technology.

Yong Cheng and Shuqing Wang contributed equally to this work.

Since its inception in the last century, laser-induced breakdown spectroscopy (LIBS) [6] technology has garnered significant attention due to its substantial advantages in material detection and characterization. This technique uses a laser as the emission source, detecting the plasma spectrum generated on the sample surface. By analyzing the characteristic emission lines of atoms and molecules, it determines the composition and properties of the sample. LIBS technology offers numerous advantages, including minimal sample preparation, rapid detection, noncontact analysis, and the ability to simultaneously analyze multiple elements. Consequently, it has been widely applied in various fields, such as mineral classification [7], and the identification and classification of explosives [8].

In the identification of microorganisms such as bacteria, LIBS has also demonstrated significant potential and achieved remarkable progress [9–11]. For instance, Multari et al. successfully differentiated *Escherichia coli*, three clones of methicillin-resistant *Staphylococcus aureus* (MRSA), and other MRSA strains using LIBS combined with blind testing [12]. They later attempted to distinguish between live pathogens and dead viruses with LIBS and found it capable of identifying various strains [13]. Barnett et al. confirmed that LIBS could be used to differentiate bacteria by analyzing the spectra obtained from intestinal *Salmonella* [14]. Wu et al. developed a sensor integrating laser-induced breakdown spectroscopy with lateral flow strips (LIBS-LFS), enabling the detection of *Staphylococcus aureus* within 10 min, with a detection limit as low as 1.6 cfu $mL^{-1}$ [15]. Diedrich, Rehse, and Palchaudhuri employed discriminant function analysis on the LIBS spectra of *Escherichia coli* and other bacteria, demonstrating its effectiveness in distinguishing different pathogens [16] and various strains of the same species [17]. Baudelet et al. analyzed five types of bacteria, including *Escherichia coli*, using femtosecond LIBS, proving that bacterial concentration can be characterized by the relative concentration of their trace mineral elements [18]. These studies collectively confirm the feasibility of LIBS in bacterial identification.

Despite the high similarity in LIBS spectra among different microorganisms, combining this technique with machine learning algorithms can overcome the challenges of distinguishing bacterial spectra and enhance the accuracy of bacterial identification [19]. Researchers typically employ machine learning algorithms to train classification models using the LIBS spectra of bacteria as input. For example, Rao et al. collected LIBS spectra from 10 microbial samples, including *Bacillus subtilis* and *Saccharomyces cerevisiae*, and successfully identified these bacteria using Random Forest (RF) and principal component analysis (PCA) algorithms, achieving an accuracy of over 90% [20]. Farias et al. used near-infrared diffuse reflectance spectra combined with PCA and K-Nearest Neighbors (KNN) algorithms, attaining 100% accuracy in identifying four types of bacteria, including Salmonella enteritidis [21]. Manzoor et al. proposed a bacterial identification method combining LIBS with neural network algorithms, successfully identifying 40 strains of bacteria responsible for infections. This method not only distinguished different strains of the same bacterial species but also achieved spectral correlation exceeding 95% [22]. These studies demonstrate that using machine learning algorithms to process bacterial spectra can significantly improve identification accuracy. However, considering the safety risks associated with close-range bacterial identification, there is a necessity for research on remote bacterial identification, focusing on remote laser excitation, weak spectral signal collection, and more sophisticated machine learning algorithms.

This study focuses on exploring the feasibility of remote bacterial species identification using LIBS with a Cassegrain reflective telescope. Multiple evaluation metrics were employed to assess the performance of different classification models.

## 2 | Experiment

### 2.1 | Sample Preparation

The experiment selected nine types of bacteria: *Escherichia coli* (*E. coli*), *Bacillus subtilis* (*B. subtilis*), *Enterococcus faecalis* (*E. faecalis*), *Pseudomonas fluorescens* (*P. fluorescens*), *Salmonella typhimurium* (*S. typhimurium*), *Bacillus thuringiensis* (*B. thuringiensis*), *Staphylococcus aureus* (*S. aureus*), *Candida albicans*, and *Bacillus megaterium* (*B. megaterium*). High-purity graphite plates were chosen as the detection substrate [23, 24].

Prior to the commencement of the experiment, inoculating loops, test tubes, and other laboratory equipment were subjected to continuous disinfection under a 394 K alcohol lamp for 20 min. Subsequently, appropriate bacteria were collected from slanted solid media using inoculating loops and inoculated onto Luria-Bertani (LB) solid media. The LB solid media were then placed in a constant temperature incubator and incubated at 37°C for 36 h to ensure the purity of the bacterial strains. Following this, colonies were retrieved from the LB solid media and transferred to liquid media for shaking culture for 12 h. Upon completion of the incubation, bacterial colonies from the liquid media were retrieved for the experiment, and their concentrations were verified to be relatively constant by measuring the OD600 values. Finally, the bacterial solution underwent three washes with ultrapure water. Subsequently, 1 mL of the bacterial solution was aspirated using a pipette and evenly spread onto the surface of the test substrate to ensure uniform distribution. The substrate was then allowed to air-dry to facilitate subsequent experimental procedures.

### 2.2 | Experimental Setup

The experimental setup for remote detection of LIBS based on a Cassegrain reflective telescope is illustrated in Figure 1. The Nd:YAG laser used (Quantel Q-smart 450) emits at a wavelength of 1064 nm with a repetition rate of 10 Hz and a single pulse energy of 80 mJ. The primary and secondary mirrors of the Cassegrain telescope have diameters of 300 and 60 mm, respectively. After passing through a beam expander, the laser is reflected into the Cassegrain telescope by a dichroic mirror. By adjusting the position of the secondary mirror, the laser is focused at a distance of 3 m from the primary mirror. The samples are placed on an x-y-z sample stage, and the stage rotation ensures that the laser irradiates different points on the sample for each shot. The fluorescence of the plasma radiation is collected by a focusing lens and guided into a four-channel spectrometer

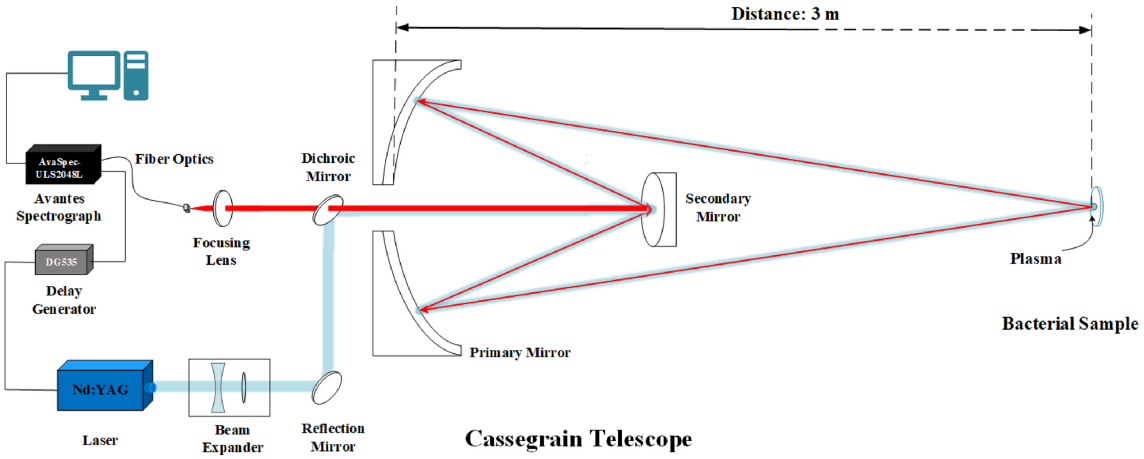


**FIGURE 1** | Experimental setup for remote bacterial identification using a Cassegrain reflective telescope-based LIBS system.

(Avantes, AvaSpec-ULS2048L). The spectrometer has an effective wavelength range of 200–1040 nm, with an integration time set to 100 ms and a delay controlled by a digital delay pulse generator (DG535) set to 300 ns. 100 spectra were collected for each bacterial sample, resulting in a total of 900 bacterial spectra collected.

## 3 | Results and Discussion

### 3.1 | Preprocessing of Bacterial Spectra

During remote detection of bacteria, the collected spectral signals exhibit high similarity due to the requirement of various basic elements such as carbon, hydrogen, nitrogen, oxygen, potassium, calcium, etc., for normal growth and metabolism of all types of bacteria. Additionally, the composition elements of the substrate and culture medium may also introduce interference to the spectra. Hence, preprocessing of the collected spectral signals is necessary.

Commonly used spectral preprocessing methods include spectral smoothing, maximum normalization, total normalization, Fourier transform, wavelength selection, derivative transformation, feature extraction, baseline correction, standard normal variate transformation, moving average smoothing, and Savitzky–Golay smoothing filter. In this study, we first filtered out bacterial spectra with a signal-to-noise ratio below 5 dB for the Na I 588.9 nm spectral line. This choice was made because, compared to other elemental lines in bacterial spectra, the Na I 588.995 nm line exhibits the most stable intensity and better signal-to-noise ratio. Subsequently, background subtraction and five-window Savitzky–Golay smoothing were applied to these spectra. The preprocessed bacterial spectra are illustrated in Figure 2, where characteristic spectral lines of each element are highlighted, and the corresponding wavelength information is listed in Table 1. These preprocessing steps aid in reducing interference and emphasizing feature signals, thereby enhancing the accuracy and reliability of subsequent analyses.

After preprocessing the bacterial spectra, we observed that different bacteria exhibit a certain degree of similarity in their spectra, yet significant differences in spectral line intensities exist. For example, both *Bacillus subtilis* and *Enterococcus faecalis* spectra display the Ca II 393.4 nm spectral line, but *Bacillus subtilis* exhibits significantly higher intensity compared to *Enterococcus faecalis*; the spectral line intensity of *Candida albicans* at Ca II 393.4 nm is much lower than at Ca II 396.8 nm. Furthermore, at Ca I 422.7 nm, only spectra of *Escherichia coli*, *Bacillus subtilis*, *Bacillus thuringiensis*, *Candida albicans*, and *Bacillus megatherium* show this spectral line, while it is not detected in spectra of other bacteria. Additionally, the intensity differences of the K I 766.5 nm, K I 769.9 nm, O I 777.2 nm, and Na I 819.5 nm spectral lines are subtle, making them difficult to distinguish accurately visually. It is noteworthy that laser energy and environmental factors also influence the intensity of bacterial spectral lines, affecting classification accuracy. Therefore, a combination of different classification algorithms is necessary to improve accuracy.

### 3.2 | Identification of Bacteria

In this study, two different classification algorithms were employed in an attempt to enhance the classification accuracy of nine types of bacteria. Additionally, model evaluation metrics including classification accuracy, recall, precision, and $F1$ score were utilized to assess the performance of these two classification models.

#### 3.2.1 | Identification by PCA

PCA is a commonly used dimensionality reduction technique employed to extract key features from high-dimensional data and compress the data [25]. It achieves this by linearly transforming the original data into a new set of variables called principal components, which are linear combinations of the original data with the highest variance. By retaining only the first few principal components, data dimensionality reduction can be achieved.

After employing PCA to reduce the dimensionality of the spectra, cumulative contribution rates of principal components for the nine bacterial strains were obtained, as shown in Figure 3. It can be observed that the cumulative contribution of the first

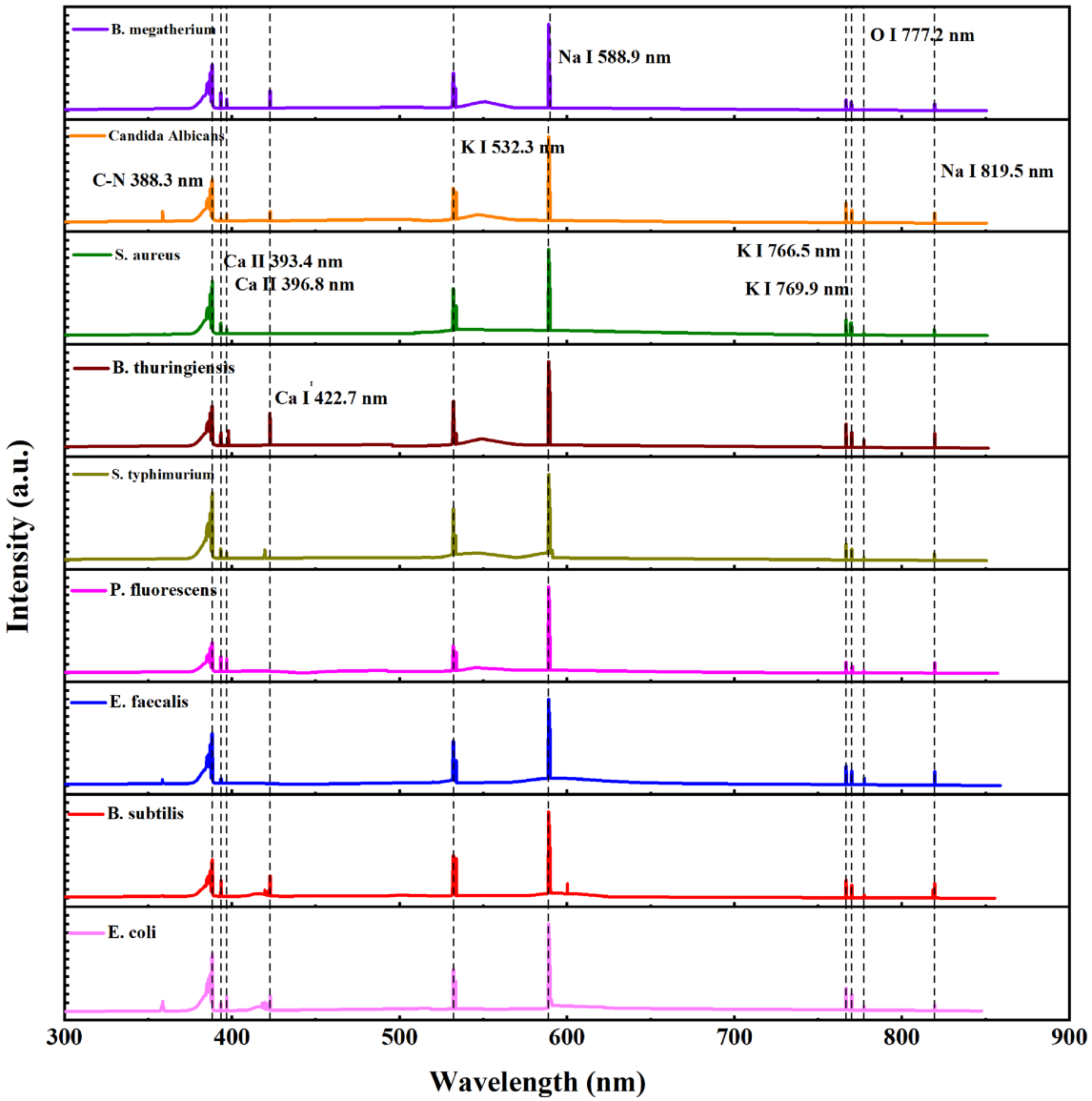


**FIGURE 2** | Averaged LIBS spectra of the nine bacterial strains after spectral preprocessing.

**TABLE 1** | Atomic and molecular emission lines observed in bacterial samples.

| No. | Element | Wavelength (nm) |
|---|---|---|
| 1 | C-N | 388.3 |
| 2 | Ca II | 393.4, 396.8 |
| 3 | Ca I | 422.7 |
| 4 | K I | 532.3, 533.9, 766.5, 769.9 |
| 5 | Na I | 588.9, 589.6, 819.5 |
| 6 | O I | 777.2 |
| 7 | N I | 818.5 |

three principal components for all nine bacterial strains exceeds 90%, indicating that these principal components are sufficient to effectively represent the compositional elements of the bacteria.

Figure 4 depicts a 3D scatter plot of the first three principal component scores for the nine bacterial strains. From the spatial stacking of data points representing various bacterial strains in the plot, it can be observed that using PCA alone does not accurately classify these nine bacterial strains [26]. Hence, it is necessary to combine other algorithms to enhance the accuracy and reliability of classification.

### 3.2.2 | Identification by SVM

Support vector machine (SVM) is a commonly used supervised learning algorithm applicable to classification and regression problems. Its basic principle is to find an optimal hyperplane in the feature space to separate samples of different classes [27]. The core idea is to maximize the margin, which means finding a hyperplane that maximizes the distance between the hyperplane and the closest support vectors. Determining the maximum margin can provide the classifier with good robustness and generalization ability, and dividing the hyperplane in high-dimensional feature

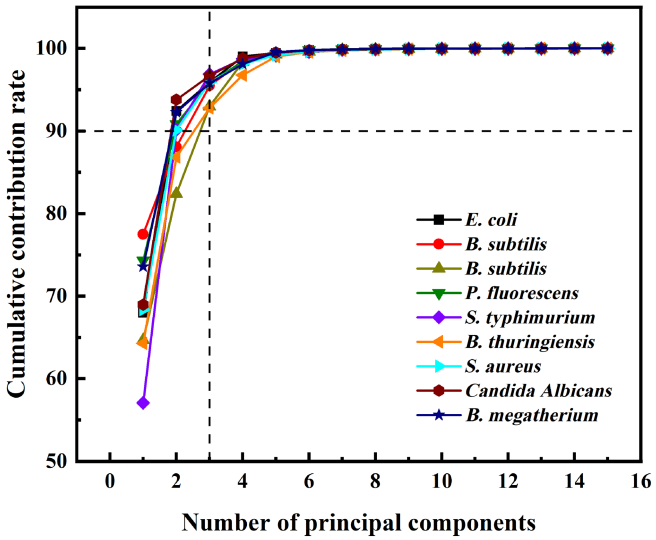


**FIGURE 3** | Cumulative contribution rates of principal component scores.

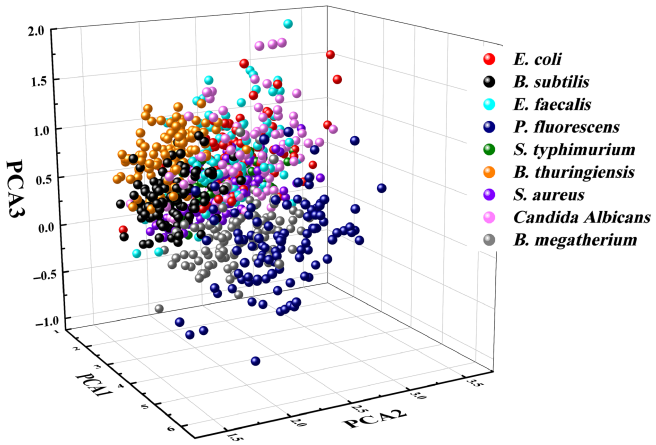


**FIGURE 4** | 3D classification plot of the nine bacterial species.

space can be used to solve nonlinear problems. However, SVM's training time can be long when dealing with large-scale datasets. SVM supports various kernel functions, including linear kernel function, polynomial kernel function, Radial Basis Function (RBF) kernel function, and Sigmoid kernel function. By using these kernel functions, data can be mapped to high-dimensional space to handle nonlinear problems. The RBF kernel function is chosen in this study because it possesses strong nonlinear modeling capabilities, enabling it to handle complex data distributions and decision boundaries. Additionally, it can map sample data to high-dimensional space, better separating different samples. These advantages contribute to improving the classification performance of the model. For this classification task, the RBF kernel parameter and penalty coefficient were optimized, resulting in an RBF kernel parameter set to 1 and a penalty coefficient set to 2.

In this bacterial identification experiment, 900 bacterial spectral data were divided into training and test sets in an 8:2 ratio. Specifically, the training set comprised 720 bacterial spectra, with 80 spectra for each type of bacterium. The test set included 180 bacterial spectra, with 20 spectra for each type of bacterium.

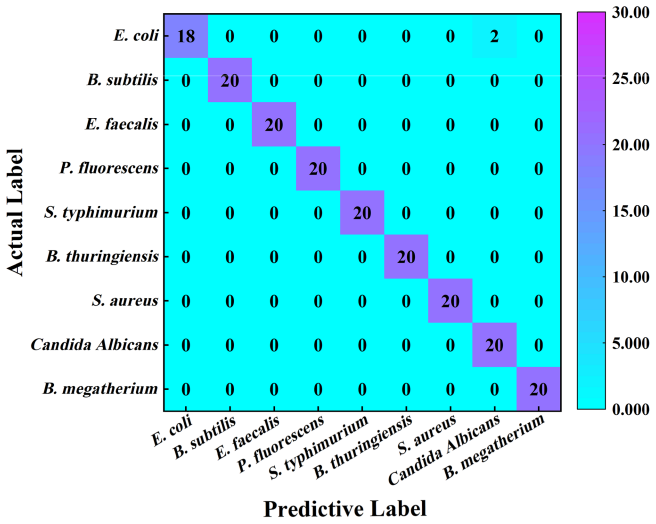


**FIGURE 5** | Confusion matrix of the SVM classification model.

The spectral data input into the machine learning model were all reduced using PCA [28]. Figure 5 shows the confusion matrix for the SVM classification model's identification of the nine bacterial strains. As shown in the figure, the SVM classification model achieved a recognition accuracy of 98.89% for the bacteria in the test set. Only two *E. coli* samples were misidentified as *Candida albicans*.

The confusion matrix is a commonly used tool for evaluating algorithm performance in classification problems. It is indispensable for tasks such as bacteria identification. It assesses algorithm performance by statistically summarizing the correct and incorrect classification results. In the confusion matrix, each row represents the situation of a particular bacteria species in the testing set, while each column represents the bacteria category predicted by the algorithm. Each element indicates the number of samples predicted to belong to a certain bacterial species. In bacteria identification tasks, the total sum of numbers in each row of the confusion matrix represents the total number of samples for that bacterial species in the testing set. The elements on the main diagonal represent the number of bacteria correctly identified, that is, the number of true positives.

By observing the confusion matrix shown in Figure 6, we can notice that the larger the elements on the main diagonal, indicating more bacteria correctly identified, the color tends toward purple. Conversely, when the number of correctly identified bacteria is low, the color tends toward cyan. The rows and columns of the confusion matrix correspond to the actual and predicted categories of bacteria, respectively. Through analysis of the confusion matrix, we can obtain the numbers of true positives, true negatives, false positives, and false negatives for each bacterial species. Based on these numbers, we can calculate some commonly used evaluation metrics for classification models, such as recall, precision, and $F1$ score, with corresponding formulas as follows:

$$\text{Recall} = \frac{\text{TP}}{\text{TP} + \text{FN}} \tag{1}$$

$$\text{Precision} = \frac{\text{TP}}{\text{TP} + \text{FP}} \tag{2}$$

$$F1\ \text{Score} = \frac{2 \times (\text{Precision} \times \text{Recall})}{\text{Precision} + \text{Recall}} \quad (3)$$

where TP, TN, FP, and FN represent true positives, true negatives, false positives, and false negatives, respectively.

### 3.2.3 | Identification by RF

RF is an ensemble learning algorithm commonly used for classification and regression tasks, which combines multiple decision trees for prediction [29]. Its basic idea is to construct multiple decision trees, each trained on a random subset of the data and using random feature subsets for splitting. Finally, the predictions from individual decision trees are aggregated to obtain the final prediction. The RF algorithm reduces overfitting by randomly selecting sample data to build decision trees, thereby improving the model's generalization ability. RF is suitable for various types of datasets and exhibits a certain level of robustness in handling missing values and outliers.

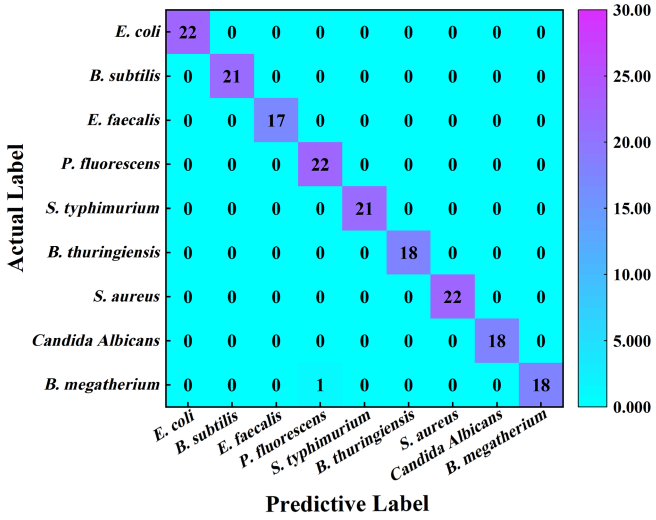


**FIGURE 6** | Confusion matrix of the RF classification model.

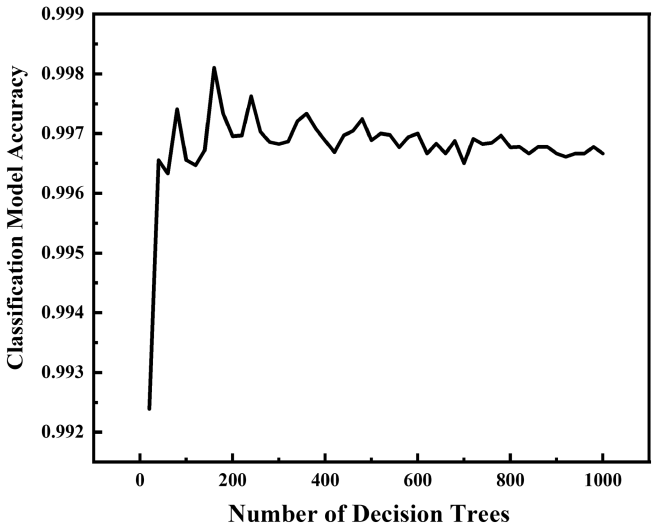


**FIGURE 7** | Impact of the number of decision trees on the classification accuracy of the RF model.

When using the RF algorithm for bacterial identification, we employed the same data as input as the SVM classification model. The training and testing sets were also divided into an 8:2 ratio. Due to the stochastic nature of the RF algorithm, a random subset of the training data is selected each time to build the classification model. Therefore, the number of spectra for different bacteria in the training and testing sets may vary.

Figure 6 shows the confusion matrix for a randomly selected test set from one of the classification tests. Upon observation, it can be seen that the classification accuracy of the RF model is 99.44%. Only one bacterial spectrum was misclassified, where *B. megatherium* was erroneously identified as *P. fluorescens*. To further evaluate the performance of the RF classification model, we conducted multiple repeated tests on the re-partitioned training set and calculated the average identification accuracy. After multiple repeated tests, the average identification accuracy reached 99.81%. In most tests, the model achieved a 100% accuracy rate, with only rare instances of misidentification of *B. subtilis* and *B. megatherium*.

To further evaluate the performance of the RF classification model, we optimized the number of decision trees in the model. Figure 7 illustrates the relationship between the number of decision trees and the classification accuracy of the RF model. It can be observed that the number of decision trees influences the accuracy of the classification model. Selecting an appropriate number of decision trees can strike a balance between model complexity, training time, memory consumption, and the effectiveness of ensemble learning, thus achieving better classifier performance and generalization ability. When the number of decision trees is less than 160, the overall trend of model performance improves as the number of decision trees increases. However, when the number of decision trees exceeds 160, further increasing the number of trees leads to fluctuations in model performance. Therefore, we ultimately selected 160 decision trees as the optimal number. This choice maintains high classification performance while avoiding issues such as prolonged classification time and reduced accuracy caused by an excessive number of decision trees, thereby achieving better generalization ability.

After finalizing the selection of 160 decision trees, we conducted multiple repeated tests on the RF model with optimized parameters. Each test was based on a re-partitioned training set, and the average identification accuracy was calculated. After multiple

**TABLE 2** | Evaluation metrics for SVM and RF classification models.

| Classification model | Classification accuracy | Recall | Precision | *F*1 score |
|---|---|---|---|---|
| SVM | 98.89% | 98.90% | 99.00% | 0.9895 |
| RF | 99.81% | 99.80% | 99.79% | 0.9979 |

tests, the average identification accuracy reached 99.81%. In most tests, the model achieved 100% accuracy, with only rare instances of misidentification of *B. subtilis* and *B. megatherium*. Table 2 presents the average evaluation metrics of the SVM and RF models from multiple repeated tests.

## 4 | Conclusions

This study designed and constructed a LIBS remote detection system based on a coaxial Cassegrain telescope, which successfully achieved effective excitation, spectral collection, and identification of bacterial species at a distance of 3 m. Considering the similarity of bacterial spectra, we compared and evaluated the predictive performance of two classification algorithms, SVM and RF, in bacterial identification. First, PCA was utilized to reduce the dimensionality of bacterial spectral data, and SVM and RF classification models were established. The SVM model, using the RBF kernel function, achieved a bacterial identification rate of 98.11% in fivefold cross-validation. The RF model, selecting 160 decision trees, achieved a bacterial identification rate of 99.81%, with corresponding recall, precision, and $F1$ score of 99.80%, 99.79%, and 0.9979, respectively, all showing improvements over the SVM model. In summary, the RF algorithm demonstrated superior performance in remotely identifying bacteria compared to SVM, proving that combining LIBS with RF can more effectively achieve remote identification of bacterial species. The bacterial identification method proposed in this study is noncontact, rapid, nondestructive, efficient, and does not produce any harmful residues, providing a safe means for detecting microorganisms in hazardous environments, with significant potential applications in medicine, public health, and other fields. In the next steps, we plan to enhance excitation efficiency using dual-pulse technology and optimize optical path design to meet the requirements of bacterial detection at greater distances.

### Author Contributions

Conceptualization: Yong Cheng, Shuqing Wang, Yan Zhang, Lei Zhang. Methodology: Yong Cheng, Shuqing Wang, Yan Zhang, Lei Zhang. Software: Yong Cheng, Shuqing Wang. Data curation: Yong Cheng, Shuqing Wang. Formal analysis: Yong Cheng, Shuqing Wang. Writing – original draft: Yong Cheng, Shuqing Wang. Writing – review and editing: Lei Zhang, Wangbao Yin. Project administration: Lei Zhang, Wangbao Yin, Suotang Jia, Liantuan Xiao. Funding acquisition: Wangbao Yin, Suotang Jia, Liantuan Xiao. Investigation: Fei Chen, Jiahui Liang. Validation: Fei Chen, Jiahui Liang. Supervision: Fei Chen, Jiahui Liang.

### Acknowledgments

The authors acknowledge support for the experimental device by the State Key Laboratory of Quantum Optics and Optical Quantum Devices at Shanxi University.

### Conflicts of Interest

The authors declare no conflicts of interest.

### Data Availability Statement

Data underlying the results presented in this paper are not publicly available at this time but may be obtained from the authors upon reasonable request.

### References

1. Z. H. Zhang, L. L. Xiao, Y. Lou, et al., "Development of a Multiplex Real-Time PCR Method for Simultaneous Detection of *Vibrio parahaemolyticus*, *Listeria monocytogenes* and *Salmonella* spp. in Raw Shrimp," *Food Control* 51 (2015): 31–36, https://doi.org/10.1016/j.foodcont.2014.11.007.

2. M. Yan, W. D. Li, Z. W. Zhou, H. X. Peng, Z. Y. Luo, and L. Xu, "Direct Detection of Various Pathogens by Loop-Mediated Isothermal Amplification Assays on Bacterial Culture and Bacterial Colony," *Microbial Pathogenesis* 102 (2017): 1–7, https://doi.org/10.1016/j.micpath.2016.10.025.

3. A. C. Vinayaka, T. A. Ngo, K. Kant, et al., "Rapid Detection of *Salmonella enterica* in Food Samples by a Novel Approach With Combination of Sample Concentration and Direct PCR," *Biosensors and Bioelectronics* 129 (2019): 224–230, https://doi.org/10.1016/j.bios.2018.09.078.

4. T. Inagaki, S. Asahi, K. Ogawa, et al., "Development of a Rapid Detection Method for the Macrolide Resistance Gene in *Mycobacterium avium* Using the Amplification Refractory Mutation System–Loop-Mediated Isothermal Amplification Method," *Microbiology Spectrum* 12 (2024): 02339, https://doi.org/10.1128/spectrum.02339-23.

5. X. R. Mei, X. W. Zhai, C. W. Lei, et al., "Development and Application of a Visual Loop-Mediated Isothermal Amplification Combined With Lateral Flow Dipstick (LAMP-LFD) Method for Rapid Detection of Salmonella Strains in Food Samples," *Food Control* 104 (2019): 9–19, https://doi.org/10.1016/j.foodcont.2019.04.014.

6. L. Brunnbauer, Z. Gajarska, H. Lohninger, and A. Limbeck, "A Critical Review of Recent Trends in Sample Classification Using Laser-Induced Breakdown Spectroscopy (LIBS)," *TrAC Trends in Analytical Chemistry* 159 (2023): 116859, https://doi.org/10.1016/j.trac.2022.116859.

7. K. C. Guo, Z. C. Wu, X. P. Zhu, et al., "Mineral Element Abundance Identification Based on LIBS Emission Line Selection by Loading Space Distance of Principal Component Analysis," *Acta Photonica Sinica* 48 (2019): 103002.

8. J. L. Gottfried, D. Lucia, C. A. Munson, and A. W. Miziolek, "Laser-Induced Breakdown Spectroscopy for Detection of Explosives Residues: A Review of Recent Advances, Challenges, and Future Prospects," *Analytical and Bioanalytical Chemistry* 395 (2009): 283–300, https://doi.org/10.1007/s00216-009-2802-0.

9. V. K. Singh, J. Sharma, A. K. Pathak, C. T. Ghany, and M. A. Gondal, "Laser-Induced Breakdown Spectroscopy (LIBS): A Novel Technology for Identifying Microbes Causing Infectious Diseases," *Biophysical Reviews* 10 (2018): 1221–1239, https://doi.org/10.1007/s12551-018-0465-9.

10. J. Kaiser, K. Novotný, M. Z. Martin, et al., "Trace Elemental Analysis by Laser-Induced Breakdown Spectroscopy—Biological Applications," *Surface Science Reports* 67 (2012): 233–243, https://doi.org/10.1016/j.surfrep.2012.09.001.

11. E. L. Yang, W. Liao, Q. Y. Lin, et al., "Quantitative Analysis of *Salmonella typhimurium* Based on Elemental-Tags Laser-Induced Breakdown Spectroscopy," *Analytical Chemistry* 92 (2022): 8090–8096, https://doi.org/10.1021/acs.analchem.9b05608.

12. R. A. Multari, D. A. Cremers, J. M. Dupre, and J. E. Gustafson, "The Use of Laser-Induced Breakdown Spectroscopy for Distinguishing Between Bacterial Pathogen Species and Strains," *Applied Spectroscopy* 64 (2010): 750–759, https://doi.org/10.1366/000370210791666183.

13. R. A. Multari, D. A. Cremers, and D. A. Bostian, "Use of Laser-Induced Breakdown Spectroscopy for the Differentiation of Pathogens and Viruses on Substrates," *Applied Optics* 51 (2012): 57–64, https://doi.org/10.1364/AO.51.000B57.

14. C. Barnett, C. Bell, K. Vig, et al., "Development of a LIBS Assay for the Detection of *Salmonella enterica* Serovar Typhimurium From Food," *Analytical and Bioanalytical Chemistry* 400 (2011): 3323–3330, https://doi.org/10.1007/s00216-011-4844-3.

15. J. Wu, Y. Liu, Y. W. Cui, X. H. Zhao, and D. M. Dong, "A Laser-Induced Breakdown Spectroscopy-Integrated Lateral Flow Strip (LIBS-LFS) Sensor for Rapid Detection of Pathogen," *Biosensors & Bioelectronics* 142 (2019): 111508, https://doi.org/10.1016/j.bios.2019.111508.

16. J. Diedrich, S. J. Rehse, and S. Palchaudhuri, "Pathogenic *Escherichia coli* Strain Discrimination Using Laser-Induced Breakdown Spectroscopy," *Journal of Applied Physics* 102 (2007): 014702, https://doi.org/10.1063/1.2752784.

17. J. Diedrich, S. J. Rehse, and S. Palchaudhuri, "*Escherichia coli* Identification and Strain Discrimination Using Nanosecond Laser-Induced Breakdown Spectroscopy," *Applied Physics Letters* 90 (2007): 163901, https://doi.org/10.1063/1.2723659.

18. M. Baudelet, J. Yu, M. Bossu, et al., "Discrimination of Microbiological Samples Using Femtosecond Laser-Induced Breakdown Spectroscopy," *Applied Physics Letters* 89 (2006): 163903, https://doi.org/10.1063/1.2361270.

19. S. J. Rehse, "A Review of the Use of Laser-Induced Breakdown Spectroscopy for Bacterial Classification, Quantification, and Identification," *Spectrochimica Acta B* 154 (2019): 50–69, https://doi.org/10.1016/j.sab.2019.02.005.

20. G. F. Rao, L. Huang, M. H. Liu, et al., "Discrimination of Microbe Species by Laser Induced Breakdown Spectroscopy," *Chinese Journal of Analytical Chemistry* 46 (2018): 1122–1128.

21. L. R. Farias, J. S. Panero, J. S. Riss, A. P. Correa, M. J. Vital, and F. D. Panero, "Rapid and Green Classification Method of Bacteria Using Machine Learning and NIR Spectroscopy," *Sensors* 23 (2023): 7336, https://doi.org/10.3390/s23177336.

22. S. Manzoor, S. Moncayo, F. N. Villoslada, et al., "Rapid Identification and Discrimination of Bacterial Strains by Laser Induced Breakdown Spectroscopy and Neural Networks," *Talanta* 121 (2014): 65–70, https://doi.org/10.1016/j.talanta.2013.12.057.

23. J. H. Liang, S. Q. Wang, W. F. Zhang, et al., "Rapid and Accurate Identification of Bacteria Utilizing Laser-Induced Breakdown Spectroscopy," *Biomedical Optics Express* 15 (2024): 1878–1891, https://doi.org/10.1364/BOE.517213.

24. Z. Q. Mi, S. Q. Wang, X. F. Ma, et al., "Study on Direct Identification of Bacteria by Laser-Induced Breakdown Spectroscopy," *Analytical Methods* 15 (2023): 297–303, https://doi.org/10.1039/D2AY01840C.

25. I. T. Jolliffe and J. Cadima, "Principal Component Analysis: A Review and Recent Developments," *Philosophical Transactions of the Royal Society A: Mathematical, Physical and Engineering Sciences* 374 (2016): 20150202, https://doi.org/10.1098/rsta.2015.0202.

26. H. R. Sun, C. R. Yang, Y. Y. Chen, Y. X. Duan, Q. W. Fan, and Q. Y. Lin, "Construction of Classification Models for Pathogenic Bacteria Based on LIBS Combined With Different Machine Learning Algorithms," *Applied Optics* 61 (2022): 6177–6185, https://doi.org/10.1364/AO.463278.

27. H. F. Wang, B. C. Zheng, S. W. Yoon, and H. S. Ko, "A Support Vector Machine-Based Ensemble Algorithm for Breast Cancer Diagnosis," *European Journal of Operational Research* 267 (2018): 687–699, https://doi.org/10.1016/j.ejor.2017.12.001.

28. Q. Q. Wang, G. Teng, X. L. Qiao, et al., "Importance Evaluation of Spectral Lines in Laser-Induced Breakdown Spectroscopy for Classification of Pathogenic Bacteria," *Biomedical Optics Express* 9 (2018): 5837–5850, https://doi.org/10.1364/BOE.9.005837.

29. L. Breiman, "Random Forests," *Machine Learning* 45 (2001): 5–32, https://doi.org/10.1007/978-1-4899-7687-1_695.